Rapid Recognition of Glucose Molecular Fingerprint Using Transmissive Microfluidic Multiplexing Metasensor

Shengyuan Shen and Lin Chen, *Member, IEEE*

***Abstract*—The multiplex metasurfaces are powerful for terahertz (THz) fingerprint enhancement. However, current technologies were still confronted with the problem of limited operating bandwidth. In this work, we introduced a broadband frequency-agile metasensor based on guided mode resonances (GMRs), which features a dual-adjustability structure and has been demonstrated to enhance and distinguish broadband absorption fingerprint spectra. Such frequency-agile dual adjustability can be achieved by both the period of the grating and the thickness of GMR waveguides integrated with a microfluidic system. This ultimately results in the collection of multiple response spectra, creating a one-to-many correspondence between spatial information and spectral information. Taking glucose molecule for example, the enhancement factor can be achieved as high as 304 times at the frequency range from 1.78 to 2.05 THz. This multiplex microfluidic metasensor has the potential for nondestructive analyte detection across a wide spectral range.**

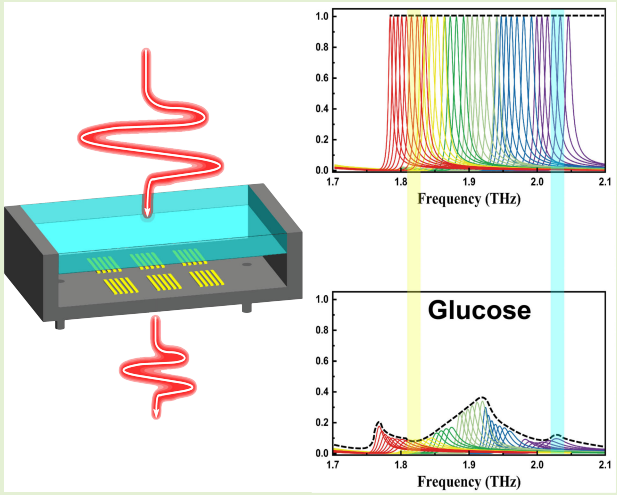

***Index Terms*— Frequency agile, guided mode resonance (GMR), metasensor, microfluidics, thickness multiplex.**

Manuscript received 19 March 2024; accepted 30 March 2024. Date of publication 8 April 2024; date of current version 15 May 2024. This work was supported in part by the Basic Science Center Project of the National Natural Science Foundation of China under Grant 61988102; in part by the National Natural Science Foundation of China under Grant 62275157; in part by Shanghai Shuguang Program, China, under Grant 18SG44; and in part by the 111 Project under Grant D18014. The associate editor coordinating the review of this article and approving it for publication was Dr. Amir Ebrahimi. *(Corresponding author: Lin Chen.)*

Shengyuan Shen is with the Terahertz Technology Innovation Research Institute, Terahertz Spectrum and Imaging Technology Cooperative, Innovation Center Shanghai Key Laboratory of Modern Optical System, University of Shanghai for Science and Technology, Shanghai 200093, China.

Lin Chen is with the Terahertz Technology Innovation Research Institute, Terahertz Spectrum and Imaging Technology Cooperative, Innovation Center Shanghai Key Laboratory of Modern Optical Systems, University of Shanghai for Science and Technology, Shanghai 200093, China, and also with Shanghai Institute of Intelligent Science and Technology, Tongji University, Shanghai 200092, China (e-mail: linchen@usst.edu.cn).

This article has supplementary downloadable material available at https://doi.org/10.1109/JSEN.2024.3384291, provided by the authors.

Digital Object Identifier 10.1109/JSEN.2024.3384291

I. Introduction

TERAHERTZ (THz) wave range covers electromagnetic wave frequency from 0.1 to 10 THz, and THz time-domain spectroscopy has been highly active in areas, such as imaging and rapid detection in recent years [1], [2], [3], [4], [5]. The principle is to use the characteristic vibration frequencies of molecules or macromolecules from THz band to quickly identify the biomolecules. To enhance light–matter interactions, numerous studies have employed metallic metasensor to achieve a significant enhancement of local electric fields [6], [7], [8], [9], [10], [11], [12]. For instance, the WaveFlex biosensors have been proposed to enhance light–matter interactions [13]. Optical fiber generally utilizes different parameters, such as wavelength, amplitude, and phase, in response to changes in refractive index (RI) and temperature. It primarily operates on the idea of enhancing localized surface plasmon resonance (LSPR) events by receiving additional evanescent waves. Based on the LSPR principle, improvement of the structure through a diversified

combination mechanism can achieve selective recognition. Recently, Kumar et al. [14] achieved high-sensitivity detection of ascorbic acid by utilizing photosensitive fiber-based sensing probe. Zhang et al. [15] provided a systematic overview of various SPR sensors. Pandey et al. [16] combined humanoid-shaped tapered optical fiber to achieve the indirect excitation of LSPR through evanescent field and detect different concentrations of histamine. In addition, if the resonance and absorption features happen to overlap in the spectrum, the near-field enhancement created by the metasensor will facilitate the interaction between molecules and resonators, resulting in significant changes in resonance linewidth and intensity [17], [18], [19], [20]. So, it provides an intuitive representation of molecular characteristics. Metasensors designed based on this principle have been widely applied in fields, such as environmental analysis and biodetection [21], [22], [23]. Nevertheless, the actual situation is still far from ideal. The resonance frequency of the unit is easily influenced by the surrounding environment and leading to irregular frequency drift, which causes a mismatch in the designed overlap [24]. Simultaneously, relying on a single characteristic fingerprint for the detection of analytes may lead to a higher occurrence of error. A recently emerged broadband absorption spectrum enhancement strategy based on multiplexing technique can be used to address this issue. The multiplexing technique is a method that detects analytes at the sensor surface by detecting the changes in electric field intensity. In this operating mechanism, two general methods are employed to obtain a range of distinct resonant peaks, thereby enhancing the interaction between electromagnetic waves and trace-level samples in the broadband frequency range. One approach adjusts the geometric parameters of the metasurface to create multiple unit cell structures, thereby forming a metasurface capable of generating a series of distinct resonant peaks [25]. Another approach involves externally manipulating metasurface under artificial conditions to obtain a resonant peak range within the metasurface composed of the same unit cell structure. For instance, this can be achieved by using graphene as a medium for electrode modulation [26]. However, the fabrication and manipulation graphene-based metasensors are huge challenges. Some reflective multiplex schemes are also achieved by adjusting the incident angle to alter phase conditions [27], [28]. While the reflective metasensors exhibit excellent performance, they have certain limitations in practical applications. For instance, due to the spatial overlap of the illumination and collection optical paths, the oblique incidence is usually preferred over normal incidence. In addition, the inevitable manual error makes the precise regulation of the incidence angle still a major challenge, which prevents the reliability and accuracy of the integration of THz systems. Moreover, ON-chip integration of the sensors used for detection tends to favor the transmissive version of devices [29].

Here, we developed an ultrabroadband frequency-multiplexed metasensor based on guided mode resonances (GMRs), which combines the periodic structure of the grating with the medium thickness adjustment mechanism of the microfluidic system to cover broadband frequency range. The multiplexing metasensors were investigated based on frequency-domain finite-element simulation. GMR is a physical effect that occurs in a grating-waveguide interaction structure [30], [31]. It offers a high transmittance and high-Q factor, which ensures trace molecular fingerprint detection in the wide THz frequency range [32], [33], [34], [35], [36]. The resonance frequency is highly related to the period of GMR metagrating. In addition, the integrated microfluidic is also introduced in GMR guiding layer to achieve frequency-agile metasensor to further expand operation frequency range. By using such active frequency-agile regulation techniques, the unique glucose molecule fingerprint with thickness of 1 μm can be amplified by 304 times with the range of 1.78–2.05 THz. Recently, Lakshmi et al. [37] proposed a glucose monitoring pressure sensor that detects glucose concentration through the resistance changes induced by pressure. This method is particularly suitable for complex scenarios, such as wearable devices. The structural approach mentioned significantly improves the accuracy and stability during the detection process. However, there are still some information of glucose fingerprint in THz range. The THz approach in this manuscript may provide complementary methods to analytical approaches proposed in [37]. This metasensor has also the potential approach for versatile miniaturized THz spectroscopy.

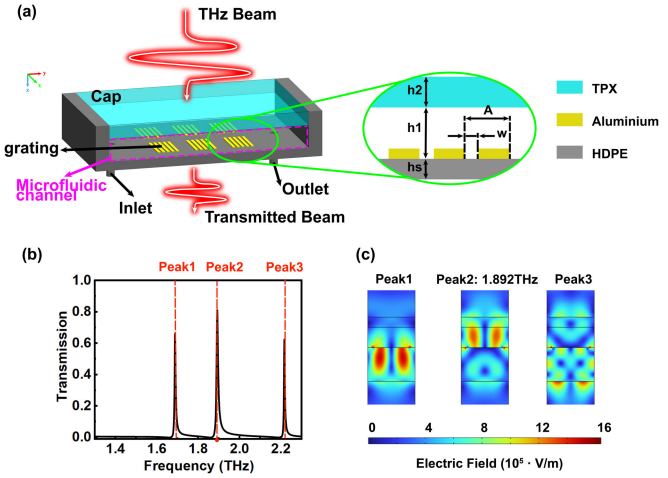

Fig. 1. (a) Schematic of the thickness-multiplexed transmissive grating. $A = 140$ μm, $w = 1$ μm, $h_1 = A/3$, $h_2 = A/5$, and $h_s = 2A/3$. (b) Transmission spectra of grating without the analyte in the range of 1–2 THz. (c) Electric field distribution of grating single-period unit at three resonance peaks.

II. Design and Method

A. Metasensor Design

The schematic of the proposed transmissive metasensor integrated microfluidic for multiplexing spectral signals was shown in Fig. 1(a). Here, h_1 and h_s denote the thickness of polymethylpentene (TPX) and polyethylene (HDPE), respectively. The microfluidic channel height h_2 can be tuned by micrometer screw (see Section I, Supporting Information). Hexadecane fluid is selected due to nearly frequency-independent refractive indices in the THz range [33]. Since materials (TPX, hexadecane, and HDPE) are used to suppress the transmission loss of THz waves, the

imaginary parts of materials are ignored, and the permittivity of TPX, hexadecane, and HDPE are $\varepsilon_1 = 1.46^2$, $\varepsilon_2 = 1.428^2$, and $\varepsilon_s = 1.6^2$, respectively [38], [39], [40].

As we know, GMR is caused by the resonant coupling of diffracted light by metal gratings and guided modes in a waveguide, which shows high-Q spectral response [41]. In order to analyze high-Q GMR modes, we perform 2-D optical simulation based on the frequency-domain finite-element method by using the commercial software COMSOL Multiphysics [42]. The unit cell of structure is adopted with periodic Floquet boundary conditions. The input THz wave is TE mode, which propagates through the grating in normal incidence [31]. The transition boundary condition is used for the aluminum layer and analytical sample. The simulation narrowband transmission spectra are shown in Fig. 1(b). There are three resonance peaks in the frequency range from 1 to 2 THz. The peak transmission is higher than 0.9. Fig. 1(c) shows the distribution of electric field intensity at three peak locations. Compared with the electric field of peak 1 and peak 3, most field intensity is localized inside substrates; electric field energy is localized around TPX cap layer as well as the channel. Since the analytes are covered on the cap (see Section I, Supporting Information), resonance peak 2 may have higher figure of merit (FoM) due to a large overlap with the analytes. The Q factor for peak 2 is over 200, and the associated FoM is 212.8. Such features would have the potential to facilitate the sensing of broadband molecular fingerprints. To demonstrate how the liquid in microfluidic channel has influence the transmission resonance, the transmission spectra for a homologous series of linear chain hydrocarbons were calculated and shown in Section II, Supporting Information. The RI difference between liquid in microfluidic layer and TPX layer (Δn) only results in the resonance frequency shift and does not affect the distortion of resonance profile. The effects of structural parameter (w) of the transmissive metasensors were also investigated in detail in Section I, Supporting Information. In general, a structure with a small slit (w) provides a distinct higher Q transmission peak. In this work, we chose $w = 1$ μm, and the duty cycle is 1/140.

B. Microfluidic Thickness and Structural Period Multiplexing

The reconfigurable properties of GMRs for the metasensor are enabled by manipulating two physical factors, including the grating period and microfluidic channel thickness. For each factor, we investigate the multiplexed mechanism. In the discussion, we adopt $\Delta n = 0.032$ (hexadecane fluid). We first focus on the thickness of microfluidic channel in the metasensor. According to the eigenvalue equation of the modulated guided mode for TE polarization

$$\tan(kd) = \frac{k(\gamma + \delta)}{k^2 - \gamma\delta} \tag{1}$$

where d is the thickness of the microfluidic layer, $k = (\varepsilon_2 k^2 - \beta^2)^{(1/2)}$, $\gamma = (\beta^2 - \varepsilon_1 k^2)^{(1/2)}$, and $\delta = (\beta^2 - \varepsilon_s k^2)^{(1/2)}$. It reveals that the microfluidic thickness condition is involved in influencing the resonant behavior of the GMR waveguide with the propagation constant β. According to (1), the thickness of the microfluidic layer plays an important role in controlling the resonance frequencies of GMRs [43]. The schematic of the principle is shown in the inset of Fig. 2(a). The active control of resonance frequency of GMR mode is achieved by varying the thickness of the microfluidic system. For instance, when we tune the thickness from 10 to 45 μm, the normalized transmission peak shifts to the low-frequency range and Q factors are in the range from 204.6 to 283.86, as observed in Fig. 2(a). Fig. 2(b) shows the relationship between resonance frequency f_0 and thickness difference Δ. The results demonstrate an approximately linear relationship between the frequency shift and Δ with thickness of microfluidic system and a slope of 1.66 GHz/μm, and the fitting equation is $y = -1.66x + 2.05883$. Therefore, we can use this linear fitting equation to determine the position of the sensor resonance frequency by varying Δ. Considering that the resolution of micrometer is 10 μm, the spectral resolution can achieve 16.6 GHz, which is sufficient to multiplexing detection.

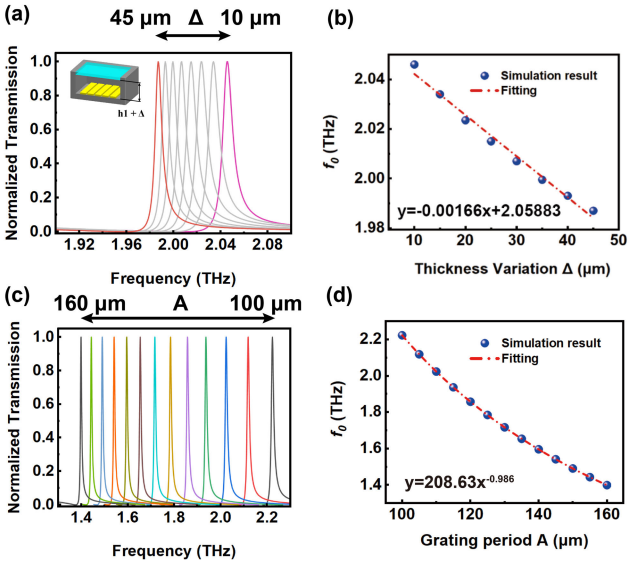

Fig. 2. (a) Normalized transmission spectra of the unit structure. (b) Corresponding tips of the resonance shift as a function of gradual Δ. (c) Numerically simulated metasensor transmission spectra for different values of structure period A. (d) Central resonance frequency with respect to the grating period *A*.

We next study another scheme of multiplexed GMRs by tuning the period (A) of metagrating with certain duty cycle. The structure period matching condition can be expressed as follows [44]:

$$\beta = k\left(\sqrt{\varepsilon_2}\frac{ic}{f_0 A}\right) \tag{2}$$

where A is the metagrating period, c is the vacuum light speed, f_0 is the peak frequency, and i is the diffraction order ($+1$ or -1). When the parameters of the grating structure meet this condition, the GMRs can be produced. For instance, if A is varied from 100 to 160 μm, the structure-resolved transmission spectra of the metasensor without analyte coating are plotted in Fig. 2(c), which can support the multiplexed GMRs

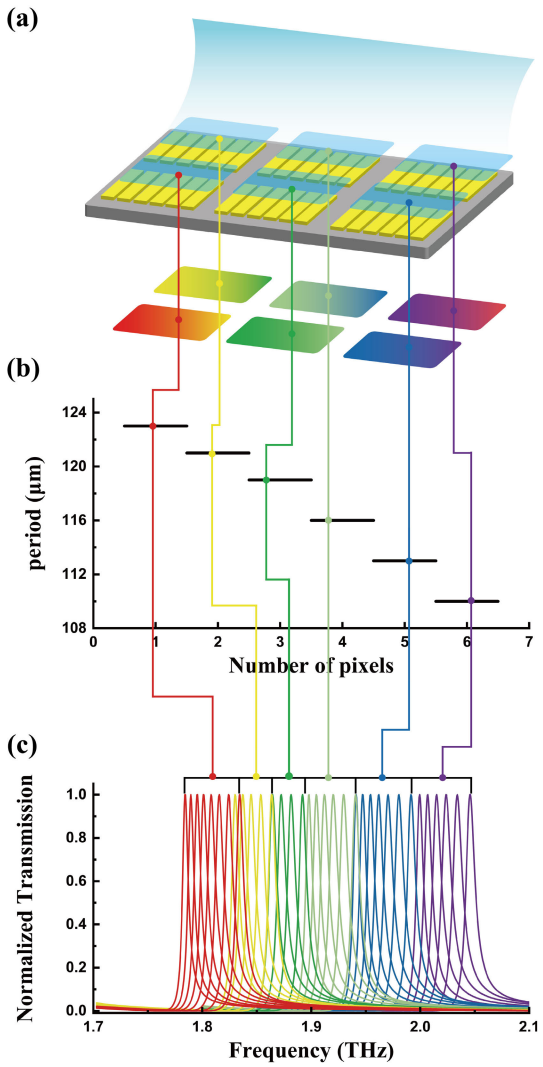

Fig. 3. (a) Regionalized metasurface composed of a microfluidic channel and different period gratings. Different unit areas correspond to unit response. (b) Periodic dimensions of the structure. Designed geometrical parameters are $A = 110$, 113, 116, 119, 121, and 123 μm, respectively. (c) Simulated normalized transmission spectra for each value of A with the gradient corresponding thickness of microfluidic channel are arranged to cover the continuous spectrum.

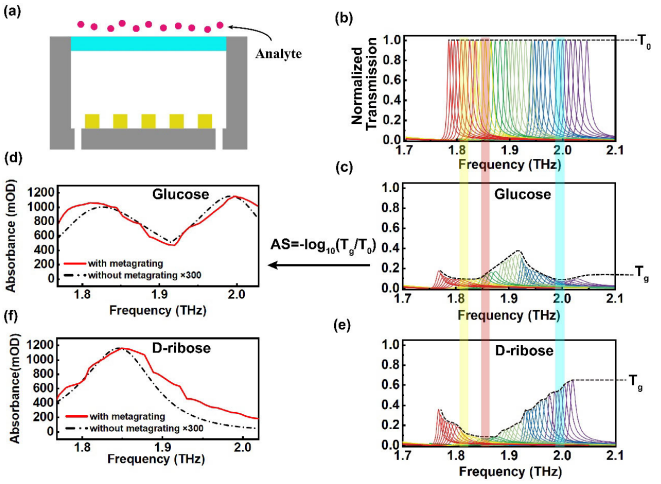

Fig. 4. (a) Schematic of the proposed metasensor with the analyze covered on the TPX surface. (b) Normalized transmission spectra in the absence of glucose with dual parameters variations. The variation periods of the gratings constituting the grating are $A = 110$, 113, 116, 119, 121, and 123 μm, respectively. Normalized transmission fingerprint retrieval mapping in the presence of 1 μm: (c) glucose and (e) D-ribose. (d) Glucose and (f) D-ribose absorption fingerprint with (red solid line) and without grating (black dashed line) were compared by 300 times magnification.

and cover a specific wide THz band. As shown in Fig. 2(d), we plot the resonance frequency as a function of the structure period. We theoretically validate the period A using (2), and it demonstrates good consistency with the simulation results. The fitting equation for this relationship is $y = 208.63x^{-0.986}$. So, the grating dimensions can be optimized for operation at the specific working frequency by using this fitting equation. Such feature contributes to extend the operating range of GMR thickness-multiplexed frequency-agile metasensor.

We continue to evaluate the performance of the two sets of multiplexed GMR-based signals by simultaneously tuning period A (the duty cycle maintains 1/140) and h_2. Here, the unit arrays of different periods with the microfluidic system are used to constitute the metasensor, as shown in Fig. 3(a). This design assigns each unit area to its specific responsive range, and the responsive ranges of adjacent units are independent and converge, forming a one-to-many mapping between spatial and spectral information. The relationship between the number of regions and grating periods is shown in Fig. 3(b). As mentioned above, the change of microfluidic system thickness can promote the adjustment of resonance frequency. The simulated transmission spectra of the metagrating structures in six exemplary unit areas with a varying A are shown in Fig. 3(c), which achieves the linear control of resonance frequency shift and covers the spectral range from 1.78 to 2.05 THz. The excellent performance lays the foundation for molecular fingerprint spectrum detection. Our design can be easily extended to larger spectral regions by changing the period parameter A with large gradients and fine-tuning the thickness of the microfluidic layer.

III. Enhancement of Glucose Fingerprint

Glucose is a commonly used analyte in the field of detection and exhibits multiple distinct absorption peak features within the range of 1–2 THz [43]. The Drude–Lorentz dispersion model as the dielectric function of glucose is adopted as follows [43]:

$$\varepsilon = \varepsilon_\infty + \sum_{j=1}^{M} \frac{f_j \omega_P^2}{\omega_{0j}^2 - \omega^2 + i\Gamma_j \omega} \tag{3}$$

where m is the number of oscillators; ω_{0j} is the resonance frequency, which determines the material's response to a specific frequency; ω_p is the plasma frequency, which determines the contribution of free charge carriers to the optical properties; f_j is the oscillator strength; ε_∞ is the relative permittivity with a high frequency; and Γ is the damping in time. We illustrate molecular fingerprint detection by covering glucose film with 1 μm on the TPX layer [Fig. 4(a)] and utilize (3) to express the properties of molecules at 1.811 and 1.996 THz. The fingerprint enhancement capability can be obtained by

TABLE I
COMPARISON RESULTS OF THE DESIGNED ENHANCING METHOD HERE WITH THE SIMILAR RESULTS

Ref	Cell structure	Analyte	Multiplexing mode	Operation range	Enhancement factor
[33] (2020)	Dielectric pair pillars	PMMA	Incident angle	Mid infrared	~50 times
[34] (2022)	Dielectric pair pillars	PMMA	Geometry	Mid infrared	~60 times
[35] (2020)	Metagrating	hBN	Incident angle	Mid infrared	~30 times
[36] (2022)	Metagrating	α-Lactose	Incident angle	THz	~20 times
[38] (2011)	Metal bars in mesh	α-Lactose	Geometry	THz	~200 times
[39] (2018)	Au coated PDMS	α-Lactose	Geometry	THz	~270 times
Our work	Metagrating	glucose	Period and microfluidic	THz	~304 times

calculating the transmission intensities of series of transmission spectra. The normalized transmission spectra before and after glucose physisorption are shown in the up and down panels of Fig. 4(b) and (c), respectively. The normalized transmission spectra have an obvious attenuation caused by the absorption characteristics of glucose [Fig. 4(c)]. According to Lambert–Beer law, the absorbance signal can be defined as $AS = -\log10(\underline{T_g}/\underline{T_0})$, where T_0 and T_g are the envelope of peak transmissivity before and after glucose absorption, respectively. The absorption characteristics of glucose molecules are revealed by calculation the absorbance signal AS, as shown in Fig. 4(d), which is in good agreement with the absorption characteristics exhibited on the HDPE substrate without the grating structure. The fingerprint absorptance is boosted nearly 304 times. An evaluation of sensitivity and limit of detection has to be demonstrated in Section III, Supporting Information. The results for D-ribose with absorption fingerprint spectra in the range of 1.7–2.1 THz are also presented in Fig. 4(e) and (f). D-ribose, a common pharmaceutical intermediate used in the production of a variety of nucleic acid drugs, exhibits a distinct absorption fingerprint spectrum in the 1.7–2.1-THz range [45]. The thicknesses of glucose and D-ribose are both 1 μm. The proposed metagrating in this work has successfully generated accurate enhanced absorption fingerprint spectra for D-ribose and glucose, resulting in the enhanced absorption fingerprint spectra for trace substances. The baseline of transmission spectra in the absence of analytes is about 0.05. When analyte is covered on the TPX surface, the normalized transmission fingerprint retrieval mapping in the presence of 1-μm glucose and D-ribose can still above the baseline and can be observed clearly (see Section IV, Supporting Information). We also note that variations in the grating period A and microfluidic layer variations Δ will affect thickness sensitivity (see Section 5, Supporting Information).

Table I provides a multiplexing performance comparison between previous works and this work. The enhancement factor is defined as $EF = AS/AS_0$, where AS and AS_0 refer to the absorbance of trace analyte on the metasensor and unpatterned sensor, respectively. The proposed microfluidic frequency-agile metasensor combined with geometric period multiplexing achieves a maximum enhancement factor of approximately 304 times at the absorption peak of the sample material, indicating that the dual-adjustability frequency-agile metasensor exhibits superior performance in detecting trace analytes and can be utilized for detecting trace analytes in the THz range.

IV. CONCLUSION

We have presented frequency-agile thickness and period multiplex THz molecular fingerprint metasensor based on GMR, which can significantly extend the operational bandwidth of the detection range. By employing dual adjustability, the metagrating and microfluidic system are combined to establish a one-to-many mapping relationship between spatial and spectral information. This ultimately can cover the THz fingerprint range. As long as the resonance frequency of the analyte achieves in the frequency-agile coverage range, the spectral fingerprint detection can be greatly improved. Furthermore, we can achieve the ability to specific recognition of analytes by expanding frequency-agile coverage range to fingerprint spectra. The simultaneously microfluidic thickness and structural periods multiplexing configuration is able to deliver potential applications in detecting molecular interactions with high enhancement. The broadband THz fingerprint spectrum obtained by this method will open up a new idea for the convenience of broadband THz functional devices. We note that there still exist some limitations. Multiplexing technology cannot be excited for the coherent coupling of a broadband mode of the metasurface to a narrowband absorption line/resonance of analyte. More recently, the absorption-induced transparency (AIT) can also achieve THz trace molecular fingerprint sensing [46]. The most intriguing characteristic of AIT is that the transmission peak, in the combined metasurface device with analyte system, appears at the spectral position where the bare analyte presents resonant absorption. Combining the AIT effect with multiplexing may improve such limitation for trace THz molecular fingerprint sensing [21].

REFERENCES

[1] N. Li et al., "Photonic crystals on copolymer film for bacteria detection," *Biosensors Bioelectron.*, vol. 41, pp. 354–358, Mar. 2013, doi: 10.1016/j.bios.2012.08.052.

[2] L. Chen et al., "Defect-induced Fano resonances in corrugated plasmonic metamaterials," *Adv. Opt. Mater.*, vol. 5, no. 8, Apr. 2017, Art. no. 1600960, doi: 10.1002/adom.201600960.

[3] M. G. Abdallah et al., "Quantification of neuropeptide Y with picomolar sensitivity enabled by guided-mode resonance biosensors," *Sensors*, vol. 20, no. 1, p. 126, Dec. 2019, doi: 10.3390/s20010126.

[4] C. C. Luo et al., "Terahertz lattice enhanced quasi-anapole immunosensor assisted by protein antibody and AuNPs," *Sensors Actuat. B, Chem.*, vol. 410, Mar. 2024, Art. no. 135628, doi: 10.1016/j.snb.2024.135628.

[5] D. Rodrigo et al., "Resolving molecule-specific information in dynamic lipid membrane processes with multi-resonant infrared metasurfaces," *Nature Commun.*, vol. 9, no. 1, Jun. 2018, Art. no. 2160, doi: 10.1038/s41467-018-04594-x.

[6] M. Gupta and R. Singh, "Terahertz sensing with optimized Q/V_{eff} metasurface cavities," *Adv. Opt. Mater.*, vol. 8, no. 16, Aug. 2020, Art. no. 1902025, doi: 10.1002/adom.201902025.

[7] L. Chen et al., "Mode splitting transmission effect of surface wave excitation through a metal hole array," *Light, Sci. Appl.*, vol. 2, no. 3, p. e60, Mar. 2013, doi: 10.1038/lsa.2013.16.

[8] A. Kumar, M. Gupta, P. Pitchappa, Y. J. Tan, N. Wang, and R. Singh, "Topological sensor on a silicon chip," *Appl. Phys. Lett.*, vol. 121, no. 1, Jul. 2022, Art. no. 011101, doi: 10.1063/5.0097129.

[9] T. C. W. Tan, E. Plum, and R. Singh, "Lattice-enhanced Fano resonances from bound states in the continuum metasurfaces," *Adv. Opt. Mater.*, vol. 8, no. 6, Mar. 2020, Art. no. 1901572, doi: 10.1002/adom.201901572.

[10] J.-A. Losman et al., "(R)-2-hydroxyglutarate is sufficient to promote leukemogenesis and its effects are reversible," *Science*, vol. 339, no. 6127, pp. 1621–1625, Mar. 2013, doi: 10.1126/science.1231677.

[11] J. Xu et al., "Terahertz microfluidic sensing with dual-torus toroidal metasurfaces," *Adv. Opt. Mater.*, vol. 9, no. 15, May 2021, Art. no. 2100024, doi: 10.1002/adom.202100024.

[12] E. V. Fedulova, M. M. Nazarov, A. A. Angeluts, M. S. Kitai, V. I. Sokolov, and A. P. Shkurinov, "Studying of dielectric properties of polymers in the terahertz frequency range," *Proc. SPIE*, vol. 8337, pp. 144–152, Mar. 2012, doi: 10.1117/12.923855.

[13] R. Singh, W. Zhang, X. Liu, B. Zhang, and S. Kumar, "WaveFlex biosensor: MXene-immobilized W-shaped fiber-based LSPR sensor for highly selective tyramine detection," *Opt. Laser Technol.*, vol. 171, Apr. 2024, Art. no. 110357.

[14] S. Kumar, R. Singh, Q. Yang, S. Cheng, B. Zhang, and B. K. Kaushik, "Highly sensitive, selective and portable sensor probe using germanium-doped photosensitive optical fiber for ascorbic acid detection," *IEEE Sensors J.*, vol. 21, no. 1, pp. 62–70, Jan. 2021.

[15] W. Zhang et al., "Humanoid shaped optical fiber plasmon biosensor functionalized with graphene oxide/multi-walled carbon nanotubes for histamine detection," *Opt. Exp.*, vol. 31, no. 7, pp. 11788–11803, Mar. 2023.

[16] P. S. Pandey, S. K. Raghuwanshi, and S. Kumar, "Recent advances in two-dimensional materials-based Kretschmann configuration for SPR sensors: A review," *IEEE Sensors J.*, vol. 22, no. 2, pp. 1069–1080, Jan. 2022.

[17] B. Han, Z. Han, J. Qin, Y. Wang, and Z. Zhao, "A sensitive and selective terahertz sensor for the fingerprint detection of lactose," *Talanta*, vol. 192, pp. 1–5, Jan. 2019, doi: 10.1016/j.talanta.2018.09.029.

[18] J. Wei et al., "Ultrasensitive transmissive infrared spectroscopy via loss engineering of metallic nanoantennas for compact devices," *ACS Appl. Mater. Interfaces*, vol. 11, no. 50, pp. 47270–47278, Nov. 2019, doi: 10.1021/acsami.9b18002.

[19] L. Chen, D.-G. Liao, X.-G. Guo, J.-Y. Zhao, Y.-M. Zhu, and S.-L. Zhuang, "Terahertz time-domain spectroscopy and micro-cavity components for probing samples: A review," *Frontiers Inf. Technol. Electron. Eng.*, vol. 20, no. 5, pp. 591–607, May 2019, doi: 10.1631/FITEE.1800633.

[20] T. C. Tan et al., "Active control of nanodielectric-induced THz quasi-BIC in flexible metasurfaces: A platform for modulation and sensing," *Adv. Mater.*, vol. 33, no. 27, Jul. 2021, Art. no. 2100836, doi: 10.1002/adma.202100836.

[21] J. Lyu, S. Shen, L. Chen, Y. Zhu, and S. Zhuang, "Frequency selective fingerprint sensor: The Terahertz unity platform for broadband chiral enantiomers multiplexed signals and narrowband molecular AIT enhancement," *PhotoniX*, vol. 4, no. 1, Sep. 2023, Art. no. 28, doi: 10.1186/s43074-023-00108-1.

[22] M. G. Abdallah et al., "Attachment and detection of biofouling yeast cells using biofunctionalized resonant sensor modality," *IEEE Sensors J.*, vol. 21, no. 5, pp. 5995–6002, Mar. 2021, doi: 10.1109/JSEN.2020.3040710.

[23] W. Fu et al., "Qualitative and quantitative recognition of volatile organic compounds in their liquid phase based on terahertz microfluidic EIT meta-sensors," *IEEE Sensors J.*, vol. 23, no. 12, pp. 12775–12784, Jun. 2023, doi: 10.1109/JSEN.2023.3268167.

[24] J. Lyu, L. Huang, L. Chen, Y. Zhu, and S. Zhuang, "Review on the terahertz metasensor: From featureless refractive index sensing to molecular identification," *Photon. Res.*, vol. 12, no. 2, pp. 194–217, Feb. 2024, doi: 10.1364/prj.508136.

[25] A. Tittl et al., "Imaging-based molecular barcoding with pixelated dielectric metasurfaces," *Science*, vol. 360, no. 6393, pp. 1105–1109, Jun. 2018, doi: 10.1126/science.aas9768.

[26] W. Tang, L. Wang, X. Chen, C. Liu, A. Yu, and W. Lu, "Dynamic metamaterial based on the graphene split ring high-Q Fano-resonnator for sensing applications," *Nanoscale*, vol. 8, no. 33, pp. 15196–15204, 2016, doi: 10.1039/C6NR02321E.

[27] Y. Xie, X. Liu, F. Li, J. Zhu, and N. Feng, "Ultra-wideband enhancement on mid-infrared fingerprint sensing for 2D materials and analytes of monolayers by a metagrating," *Nanophotonics*, vol. 9, no. 9, pp. 2927–2935, Jul. 2020, doi: 10.1515/nanoph-2020-0180.

[28] Y. Xie et al., "Dual-degree-of-freedom multiplexed metasensor based on quasi-BICs for boosting broadband trace isomer detection by THz molecular fingerprint," *IEEE J. Sel. Topics Quantum Electron.*, vol. 29, no. 5, pp. 1–10, Sep. 2023, doi: 10.1109/JSTQE.2023.3236981.

[29] A. Shakoor et al., "Plasmonic sensor monolithically integrated with a CMOS photodiode," *ACS Photon.*, vol. 3, no. 10, pp. 1926–1933, Sep. 2016, doi: 10.1021/acsphotonics.6b00442.

[30] Z. S. Liu and R. Magnusson, "Concept of multiorder multimode resonant optical filters," *IEEE Photon. Technol. Lett.*, vol. 14, no. 8, pp. 1091–1093, Aug. 2002, doi: 10.1109/LPT.2002.1021979.

[31] A. Sharon, H. G. Weber, H. Engel, D. Rosenblatt, A. A. Friesem, and R. Steingrueber, "Light modulation with resonant grating–waveguide structures," *Opt. Lett.*, vol. 21, no. 19, pp. 1564–1566, Oct. 1996, doi: 10.1364/ol.21.001564.

[32] S. Joseph, S. Pandey, S. Sarkar, and J. Joseph, "Bound states in the continuum in resonant nanostructures: An overview of engineered materials for tailored applications," *Nanophotonics*, vol. 10, no. 17, pp. 4175–4207, Nov. 2021, doi: 10.1515/nanoph-2021-0387.

[33] S. Joseph, S. Sarkar, and J. Joseph, "Grating-coupled surface plasmon-polariton sensing at a flat metal-analyte interface in a hybrid-configuration," *ACS Appl. Mater. Interfaces*, vol. 12, no. 41, pp. 46519–46529, Oct. 2020, doi: 10.1021/acsami.0c12525.

[34] S. Joseph, S. Sarkar, and J. Joseph, "High-sensitivity resonant cavity modes excited in a low contrast grating layer with large aspect-ratio," *IEEE Sensors J.*, vol. 22, no. 17, pp. 16856–16861, Sep. 2022, doi: 10.1109/JSEN.2022.3189182.

[35] C. Chen and J. Wang, "Optical biosensors: An exhaustive and comprehensive review," *Analyst*, vol. 145, no. 5, pp. 1605–1628, Mar. 2020, doi: 10.1039/c9an01998g.

[36] S. Pandey, N. Baburaj, S. Joseph, and J. Joseph, "Resonant optical modes in periodic nanostructures," *ISSS J. Micro Smart Syst.*, vol. 11, no. 1, pp. 113–137, Feb. 2022, doi: 10.1007/s41683-021-00087-0.

[37] G. S. Lakshmi, S. R. Karumuri, G. S. Kondavitee, and A. Lay-Ekuakille, "Design and performance analysis of a microbridge and microcantilever-based MEMS pressure sensor for glucose monitoring," *IEEE Sensors J.*, vol. 23, no. 5, pp. 4589–4596, Mar. 2023.

[38] V. Astley, K. S. Reichel, J. Jones, R. Mendis, and D. M. Mittleman, "Terahertz multichannel microfluidic sensor based on parallel-plate waveguide resonant cavities," *Appl. Phys. Lett.*, vol. 100, no. 23, Jun. 2012, Art. no. 231108, doi: 10.1063/1.4724204.

[39] L. Liang et al., "Unity integration of grating slot waveguide and microfluid for terahertz sensing," *Laser Photon. Rev.*, vol. 12, no. 11, Nov. 2018, Art. no. 1800078, doi: 10.1002/lpor.201800078.

[40] S. Han, M. V. Rybin, P. Pitchappa, Y. K. Srivastava, Y. S. Kivshar, and R. Singh, "Guided-mode resonances in all-dielectric terahertz metasurfaces," *Adv. Opt. Mater.*, vol. 8, no. 3, Sep. 2019, Art. no. 1900959, doi: 10.1002/adom.201900959.

[41] A. F. Kaplan, T. Xu, and L. Jay Guo, "High efficiency resonance-based spectrum filters with tunable transmission bandwidth fabricated using nanoimprint lithography," *Appl. Phys. Lett.*, vol. 99, no. 14, Oct. 2011, Art. no. 143111, doi: 10.1063/1.3647633.

[42] M. Abutoama and I. Abdulhalim, "Self-referenced biosensor based on thin dielectric grating combined with thin metal film," *Opt. Exp.*, vol. 23, no. 22, pp. 28667–28682, Oct. 2015, doi: 10.1364/oe.23.028667.

[43] P. Sun and Y. Zou, "Complex dielectric properties of anhydrous polycrystalline glucose in the terahertz region," *Opt. Quantum Electron.*, vol. 48, no. 1, pp. 1–10, Jan. 2016, doi: 10.1007/s11082-015-0273-4.

[44] S. S. Wang and R. Magnusson, "Theory and applications of guided-mode resonance filters," *Appl. Opt.*, vol. 32, no. 14, pp. 2606–2613, May 1993, doi: 10.1364/ao.32.002606.

[45] M. Ge, H. Zhao, T. Ji, X. Yu, W. Wang, and W. Li, "Terahertz time-domain spectroscopy of some pentoses," *Sci. China Ser. B*, vol. 49, no. 3, pp. 204–208, Jun. 2006.

[46] L. Huang et al., "Terahertz reconfigurable metasensor for specific recognition multiple and mixed chemical substances based on AIT fingerprint enhancement," *Talanta*, vol. 269, Mar. 2024, Art. no. 125481, doi: 10.1016/j.talanta.2023.125481.

Shengyuan Shen received the B.S. degree in applied physics from Yanshan University, Hebei, China, in 2020. He is currently pursuing the M.S. degree in optical engineering with the University of Shanghai for Science and Technology, Shanghai, China.

His research interests include the design of tunable terahertz metamaterial sensors.

Lin Chen (Member, IEEE) received the B.S. and M.S. degrees in electrical engineering from Southeast University, Jiangsu, China, in 2002 and 2005, respectively, and the Ph.D. degree in optics from Shanghai Jiao Tong University, Shanghai, China, in 2008.

From 2007 to 2008, he was with Avanex Corporation, Shanghai, as a Senior Engineer. From 2012 to 2013, he was a Visiting Scholar with the State Key Laboratory of Millimeter Waves, Southeast University. From 2015 to 2016, he was a Visiting Researcher with the Ultrafast THz Optoelectronic Laboratory, Oklahoma State University, Stillwater, OK, USA. At present, he has published more than 70 peer-reviewed papers with more than 3500 citations and an H-index of 26 (including five highly cited papers) in Science Citation Indexed journal, such as Light: Science and Applications. He has also applied for more than 40 invention patents, 21 authorized, and one U.S. patent.

Dr. Chen was designated Shanghai "Dawn Scholar," "Chengguang Scholar," "Top-Notch Young Talents," "Rising Star," "Pujiang Talent," and other talent titles. He also received the Publons Peer Review Award in 2018 and 2019. As the first person in charge, he has undertaken a number of national level projects, including the National Key Research and Development Plan "Major Scientific Instrument and Equipment Development" (Chief Scientist), two national major instrument projects (project), National Natural Foundation of China (general and Youth), and several projects in Shanghai. He is currently an Editorial Board Member of Frontiers in Physics, a Guest Editor, and a Corresponding Expert of Frontiers of Information Technology and Electronic Engineering.